Am J Transl Res 2018;10(9):2781-2795
www.ajtr.org /ISSN:1943-8141/AJTR0079619

Original Article

Role of double knockdown of tPA and MMP-9 on regulating the left ventricular function and remodeling followed by transverse aortic constriction-induced hypertrophic cardiomyopathy in mice

Pei-Hsun Sung[1,6], Sarah Chua[1], Kuan-Hung Chen[2], Cheuk-Kwan Sun[4], Yi-Chen Li[1], Chi-Ruei Huang[1], Chi-Wen Luo[1], Han-Tan Chai[1], Hung-I Lu[3*], Hon-Kan Yip[1,5,6,7,8*]

[1]Division of Cardiology, Department of Internl Medicine, [2]Department of Anesthesiology, [3]Division of Thoracic and Cardiovascular Surgery, Department of Surgery, Kaohsiung Chang Gung Memorial Hospital and Chang Gung University College of Medicine, Kaohsiung 83301, Taiwan; [4]Department of Emergency Medicine, E-Da Hospital, I-Shou University School of Medicine for International Students, Kaohsiung 82445, Taiwan; [5]Institute for Translational Research in Biomedicine, [6]Center for Shockwave Medicine and Tissue Engineering, Kaohsiung Chang Gung Memorial Hospital, Kaohsiung 83301, Taiwan; [7]Department of Medical Research, China Medical University Hospital, China Medical University, Taichung 40402, Taiwan; [8]Department of Nursing, Asia University, Taichung 41354, Taiwan. [*]Equal contributors.

Received May 14, 2018; Accepted August 9, 2018; Epub September 15, 2018; Published September 30, 2018

Abstract: This study tested the hypothesis that extracellular matrix accumulation in $tPA^{-/-}/MMP\text{-}9^{-/-}$ [double-knockout (DKO)] may be protective against left ventricular (LV) remodeling and dysfunction following transverse aortic constriction (TAC)-induced hypertrophic cardiomyopathy in mice. Wild-type C57BL/6 mice (n = 20) were equally categorized into sham-control (SC^1) and TAC^1. Similarly, DKO mice (n = 20) were equally divided into two groups (i.e., SC^2 and ATC^2). By days 28/60 after TAC, LV ejection fraction (LVEF) was significantly higher in TAC^2 than TAC^1, whereas LV end-systolic/diastolic dimensions displayed an opposite pattern to LVEF between the two groups (all $P < 0.05$). By day 90, LVEF was significantly higher in SC groups than that in TAC^1 and TAC^2 without notable difference between the latter two groups, whereas LV end-systolic/diastolic dimensions, cardiomyocyte size and right-ventricular systolic pressure showed an opposite pattern compared with LVEF in all groups (all $P < 0.01$). Total heart weight was highest in TAC^1 and significantly higher in TAC^2 than those in the SC groups ($P < 0.01$). LV myocardial protein expressions of inflammation (TNF-α/NF-κβ), apoptosis (mitochondrial-Bax/cleaved caspase-3/PARP), oxidative stress (NOX-1/NOX-2/oxidized protein), fibrosis (Smad3/TGF-β), DNA/mitochondrial damage (γ-H2AX/cytosolic-cytochrome-C) and LV hypertrophy/pressure-overload (β-MHC/BNP) biomarkers were significantly increased in TAC^2 compared to TAC^1 and SC groups, and significantly increased in TAC^1 compared to SC groups (all $P < 0.001$). Histopathology demonstrated that the fibrotic/collagen-deposition areas and sarcomere length exhibited an identical pattern to inflammation among the four groups (all $P < 0.0001$). In conclusion, although $tPA^{-/-}/MMP\text{-}9^{-/-}$ seemed to preserve cardiac function in an experimental setting of hypertrophic cardiomyopathy at an early stage, it failed to exert long-term protective effect.

Keywords: Double knockout mice, transverse aortic constriction, hypertrophic cardiomyopathy, heart function

Introduction

Cardiac remodeling refers to molecular, cellular and interstitial changes of the myocardium, as well as alterations in size, shape and function of the heart in response to changing loading conditions [1-4]. Cardiac remodeling represents the final common pathway of different heart diseases and is recognized as a crucial aspect of cardiac and myocardial dysfunction and a well-established determinant of the clinical course of heart failure (HF) [1-6]. Left ventricular (LV) remodeling has been reported to occur and propagate in a variety of heart diseases such as hypertrophic cardiomyopathy (HCM) [4], dilated cardiomyopathy (DCM) [7, 8], myocardial infarction (MI) and chronic ischemic heart disease [5, 6]. Not only is LV remodeling a significant parameter for predicting LV functional deterioration, but it is also an important clini-

cal indicator of long-term poor prognostic outcome in HF patients [9-11].

Abundant data have revealed that myocardium of the failing heart commonly undergoes number of structural alterations, most notably hypertrophy of cardiac myocytes and an increase in extracellular matrix (ECM), often seen as primary fibrosis. Studies have further shown that interstitial fibrosis and excessive accumulation of ECM play a crucial role in regulating LV remodeling [12-18]. Additionally, not only has fibrosis in HCM been found to be associated with impaired cardiac function and HF, but it has also been considered a key substrate for ventricular arrhythmias and sudden death [12]. However, the molecular triggers underpinning ECM production are not well established. In addition, although a recent study has demonstrated that elevated levels of matrix metalloproteinases (MMPs) are related to LV remodeling and poor prognosis in patients with HCM [17], the mechanism through which MMPs modulate LV remodeling and their role in the development of HF remain unclear in patients with HCM, DCM and ischemic heart disease. Interestingly, our recent study has demonstrated that the extent of brain infarct was remarkably reduced in MMP-9$^{-/-}$ mice compared with that in wide-type animals in the setting of ischemic stroke [19]. We have also shown that tissue plasminogen activator (tPA) plays a key role in MMP-9 activation which causes degradation of ECM, thereby facilitating the migration of endothelial progenitor cells (EPCs) to the distant zone [20]. Since the Laplace's Law states that wall stress is proportional to radius^4 (r^4), we hypothesized that tPA$^{-/-}$/MMP-9$^{-/-}$-induced ECM accumulation and LV chamber size reduction may protect the heart from LV remodeling and preserve cardiac function in the setting of TAC-induced hypertrophic cardiomyopathy in a murine model.

Materials and methods

Ethics

All animal procedures were approved by the Institute of Animal Care and Use Committee at Kaohsiung Chang Gung Memorial Hospital (Affidavit of Approval of Animal Use Protocol No. 2016092701) and performed in accordance with the Guide for the Care and Use of Laboratory Animals.

Animals were housed in an Association for Assessment and Accreditation of Laboratory Animal Care International (AAALAC; Frederick, MD, USA)-approved animal facility in our hospital with free access to water and standard animal chow and controlled temperature at 24°C and 12-hour light-dark cycles.

Animal grouping

Pathogen-free, 12-week old adult male wild-type C57BL/6 (B6) mice (n = 20) weighing 32-35 g (Charles River Technology, BioLASCO, Taiwan) were equally categorized into sham-control (SC^1) and transverse aortic constriction (TAC^1). Additionally, the tPA$^{-/-}$/MMP-9$^{-/-}$ double knockout (DKO) mice (n = 20) were equally categorized into SC^2 and TAC^2.

In the present study, 10 animals in each group were utilized for echocardiographic study. Additionally, 4 animals in each group for cross-section of whole heart for H.E. stain. On the other hand, 6 animals in each group underwent experimental studies. To generate the double knockout mice without MMP-9 and tPA expression, tPA knockout mice (tPA$^{-/-}$) were crossed to MMP-9 knockout mice (MMP-9$^{-/-}$). Concomitant genetic disruption and protein depletion of the two genes were verified by PCR-based genotyping and Western blotting. In the current study, tPA$^{-/-}$/MMP-9$^{-/-}$ DKO mice were obtained by mating of tPA$^{-/-}$ mice and MMP-9$^{-/-}$ mice (Charles River Technology, BioLASCO Taiwan Co., Ltd., Taiwan) in AAALAC at our institute.

Procedure of TAC for induction of pathological hypertrophic cardiomyopathy

The procedure and protocol have been described in our previous report [20]. In details, the mice were anesthetized with inhalational 2.0% isoflurane. Atropine 0.05 mg/kg was administered subcutaneously. A core body temperature of about 37°C was maintained during surgery by continuous monitoring with a rectal thermometer and automatic heating blanket. The mice were endotracheally intubated with positive-pressure ventilation using 100% oxygen with a tidal volume of 250 μL at a rate of 120 breaths per minute using a small animal ventilator (SAR-830/A, CWE, Inc., USA). After opening the chest wall through upper sternotomy, the aorta was carefully iden-

tified. A 25# needle was placed on the aorta on which a 7-0 prolene ligation was placed between the right and left common carotid arteries. The needle was then carefully removed, and the aortic constriction was created. After the procedure, the wound was closed, and the animal was allowed to recover from anesthesia in a portable animal intensive care unit (ThermoCare®) for 24 hours.

LV functional assessment by echocardiography

The procedure and protocol were based on our previous report [21]. In details, transthoracic echocardiography (Vevo 2100, Visualsonics, Toronto, Ontario, Canada) was performed in animals from each group prior to and at days 28, 60 ND 90 after TCA induction by a cardiologist blinded to the experimental design. M-mode standard two-dimensional (2D) left parasternal long axis echocardiographic examination was conducted. Left ventricular internal dimensions [i.e., left ventricular end-systolic diameter (LVESd) and left ventricular end-diastolic diameter (LVEDd)] were measured at mitral valve and papillary levels of the left ventricle, as per the American Society of Echocardiography (Morrisville, NC) leading-edge methodology, using at least three consecutive cardiac cycles. Left ventricular ejection fraction (LVEF) was calculated as follows: LVEF (%) = $[(LVEDd^3\text{-}LVESd^3)/LVEDd^3] \times 100\%$.

Assessment of right ventricular blood pressure and heart specimen preparation

The procedure and protocol were based on our previous report [20, 22, 23]. In details, on day 90 after TAC induction, the mice were anesthetized with inhalational 2.0% isoflurane. Each animal was endotracheally intubated with positive pressure ventilation using 100% oxygen with a tidal volume of 250 μL at a rate of 120 breaths per minute using a small animal ventilator (SAR-830/A, CWE, Inc., USA). The heart was exposed by left thoracotomy. A sterile 20-gauge, soft plastic needle was inserted into the right ventricle of each mouse to measure the right ventricular systolic pressure (RVSP). The pressure signals were first transmitted to pressure transducers (UFI, model 1050, CA, U.S.A.) and were then exported to a bridge amplifier (ML866 PowerLab 4/30 Data Acquisition Systems. ADInstruments Pty Ltd., Castle Hill, NSW, Australia) where the signals were amplified and digitized. The data were recorded and later analyzed with the Labchart software (ADInstrument). After hemodynamic measurements, the mice were euthanized, and the heart specimens were harvested.

Western blot analysis

The procedure and protocol for Western blot analysis were based on our recent reports [20, 24, 25]. Briefly, equal amounts (50 μg) of protein extracts were loaded and separated by SDS-PAGE using acrylamide gradients. After electrophoresis, the separated proteins were transferred electrophoretically to a polyvinylidene difluoride (PVDF) membrane (GE, UK). Nonspecific sites were blocked by incubating the membrane in blocking buffer [5% nonfat dry milk in T-TBS (TBS containing 0.05% Tween 20)] overnight. The membranes were incubated with the indicated primary antibodies [caspase 3 (1:1000, Cell Signaling), Poly (ADP-ribose) polymerase (PARP) (1:1000, Cell Signaling), nuclear factor (NF)-κB (1:600, Abcam), tumor necrosis factor (TNF)-α (1:1000, Cell Signaling), cytosolic cytochrome C (1:1000, BD), mitochondrial cytochrome C (1:1000, BD), phosphorylated (p)-Smad3 (1:1000, Cell Signaling), transforming growth factor (TGF)-b (1:500, Abcam), NOX-1 (1:1500, Sigma), NOX-2 (1:750, Sigma), γ-H2AX (1:1000, Cell Signaling), matrix metalloproteinase (MMP)-2 (1:1000, Abcam), MMP-9 (1:1000, Abcam), tissue inhibitors of metalloproteinase (TIMP)-2 (1:1000, Abcam), brain natriuretic peptide (BNP) (1:500, Abcam), α-MHC (1:300, Santa Cruz), β-MHC (1:1000, Santa Cruz), COX-IV (1:3000, Abcam), and Actin (1:5000, Millipore)] for 1 hour at room temperature. Horseradish peroxidase-conjugated anti-rabbit immunoglobulin IgG (1:2000, Cell Signaling, Danvers, MA, USA) was used as a secondary antibody for one-hour incubation at room temperature. The washing procedure was repeated eight times within one hour. Immunoreactive bands were visualized by enhanced chemiluminescence (ECL; Amersham Biosciences, Amersham, UK) and exposed to Biomax L film (Kodak, Rochester, NY, USA). For the purpose of quantification, ECL signals were digitized using Labwork software (UVP, Waltham, MA, USA).

Immunohistochemical (IHC) and immunofluorescent (IF) staining

The procedure and protocol of IHC and IF staining have been described in detail in our previ-

Table 1. Time courses of transthoracic echocardiographic finding among the four groups

Variables	SC[1] (n = 10)	SC[2] (n = 10)	TAC[1] (n = 10)	TAC[2] (n = 10)	*p*-value
At day 0					
LVEF (%)	61.4 ± 2.4	63.0 ± 2.4	62.7 ± 3.8	63.3 ± 2.0	> 0.5
FS (%)	32.5 ± 1.7	33.5 ± 1.7	33.5 ± 2.7	34.2 ± 1.4	> 0.5
LVEDd (mm)	3.93 ± 0.24	3.89 ± 0.31	4.03 ± 0.22	3.95 ± 0.30	> 0.5
LVESd (mm)	2.65 ± 0.16	2.64 ± 0.17	2.68 ± 0.08	2.68 ± 0.31	> 0.5
IVS thickness (mm)	0.59 ± 0.02	0.62 ± 0.07	0.59 ± 0.07	0.60 ± 0.08	> 0.5
PW thickness (mm)	0.57 ± 0.03	0.59 ± 0.04	0.59 ± 0.04	0.58 ± 0.05	> 0.5
At day 28					
LVEF (%)*	61.4 ± 2.4[a]	63.0 ± 2.4[a]	34.90 ± 6.02[b]	54.16 ± 9.50[c]	< 0.0001
FS (%)*	32.5 ± 1.7[a]	33.5 ± 1.7[a]	16.63 ± 3.07[b]	27.92 ± 6.05[c]	< 0.0001
LVEDd (mm)*	3.93 ± 0.24[a]	3.89 ± 0.31[a]	4.54 ± 0.51[b]	4.03 ± 0.33[a]	< 0.001
LVESd (mm)*	2.65 ± 0.16[a]	2.64 ± 0.17[a]	3.80 ± 0.57[b]	2.92 ± 0.43[a]	< 0.01
IVS thickness (mm)*	0.59 ± 0.02[a]	0.62 ± 0.07[a]	0.77 ± 0.14[b]	0.80 ± 0.11[b]	< 0.01
PW thickness (mm)*	0.57 ± 0.03[a]	0.59 ± 0.04[a]	0.76 ± 0.11[b]	0.71 ± 0.06[b]	< 0.001
At day 60					
LVEF (%)*	61.4 ± 2.4[a]	63.0 ± 2.4[a]	36.9 ± 10.4[b]	47.0 ± 7.2[c]	< 0.0001
FS (%)*	32.5 ± 1.7[a]	33.5 ± 1.7[a]	17.9 ± 5.3[b]	23.3 ± 4.1[c]	< 0.0001
LVEDd (mm)*	3.93 ± 0.24[a]	3.89 ± 0.31[a]	4.59 ± 0.59[b]	4.08 ± 0.53[c]	< 0.01
LVESd (mm)*	2.65 ± 0.16[a]	2.64 ± 0.17[a]	3.80 ± 0.76[b]	3.14 ± 0.53[c]	< 0.001
IVS thickness (mm)*	0.59 ± 0.02[a]	0.62 ± 0.07[a]	0.77 ± 0.08[b]	0.81 ± 0.10[b]	< 0.01
PW thickness (mm)*	0.57 ± 0.03[a]	0.59 ± 0.04[a]	0.78 ± 0.07[b]	0.75 ± 0.08[b]	< 0.001
At day 90					
LVEF (%)*	61.4 ± 2.4[a]	63.0 ± 2.4[a]	42.6 ± 11.0[b]	43.3 ± 13.4[b]	< 0.0001
FS (%)*	32.5 ± 1.7[a]	33.5 ± 1.7[a]	21.0 ± 5.7[b]	21.5 ± 7.1[b]	< 0.0001
LVEDd (mm)*	3.93 ± 0.24[a]	3.89 ± 0.31[a]	4.37 ± 0.52[b]	4.21 ± 0.44[b]	< 0.05
LVESd (mm)*	2.65 ± 0.16[a]	2.64 ± 0.17[a]	3.48 ± 0.70[b]	3.27 ± 0.51[b]	< 0.01
IVS thickness (mm)*	0.59 ± 0.02[a]	0.62 ± 0.07[a]	1.0 ± 0.10[b]	0.92 ± 0.10[b]	< 0.01
PW thickness (mm)*	0.57 ± 0.03[a]	0.59 ± 0.04[a]	0.96 ± 0.9[b]	0.83 ± 0.10[b]	< 0.01

Data was expressed as mean ± standard deviation (SD). Abbreviations: IVS = interventricular septum; LVEDd = Left ventricular end-diastolic internal dimension; LVEDs = Left ventricular end-systolic internal dimension; LVEF = Left ventricular ejection fraction; FS = Fractional shortening. Independent t test was performed for comparison of continuous variables between two groups. SC[1] = sham control in wild-type B6 mice; SC[2] = tPA$^{-/-}$/MMP-9$^{-/-}$ [i.e., double-knockout-mice (DKO)]; TAC[1] = transverse aortic constriction in wild-type B6 mice; TAC[2] = transverse aortic constriction in DKO mice. *Indicated the data were expressed as the baseline variables. Letters ([a, b, c]) indicate significant difference (at 0.05 level) by Tukey multiple comparison procedure.

ous reports [20, 24, 25]. For IHC and IF staining, rehydrated paraffin sections were first treated with 3% H_2O_2 for 30 minutes and incubated with Immuno-Block reagent (BioSB, Santa Barbara, CA, USA) for 30 minutes at room temperature. Sections were then incubated with primary antibodies specifically against γ-H2AX (1:500, Abcam), Sirius red (Sigma-Aldrich), Masson's trichrome (ScyTek Lab) and sarcomere (1:500, Imgenx), while sections incubated with the use of irrelevant antibodies served as controls. Three sections of heart specimen from each mouse were analyzed. For quantification, three randomly selected HPFs (200 × for IF studies) were analyzed in each section.

Assessment of oxidative stress

The procedure and protocol for evaluating the protein expression of oxidative stress have been described in details in our previous reports [20, 24, 25]. The Oxyblot Oxidized Protein Detection Kit was purchased from Chemicon, Billerica, MA, USA (S7150). DNPH derivatization was carried out on 6 μg of protein for 15 minutes according to the manufacturer's instructions. One-dimensional electrophoresis was carried out on 12% SDS/polyacrylamide gel after DNPH derivatization. Proteins were transferred to nitrocellulose membranes that were then incubated in the primary antibody solution (anti-DNP 1:150) for 2 hours, followed

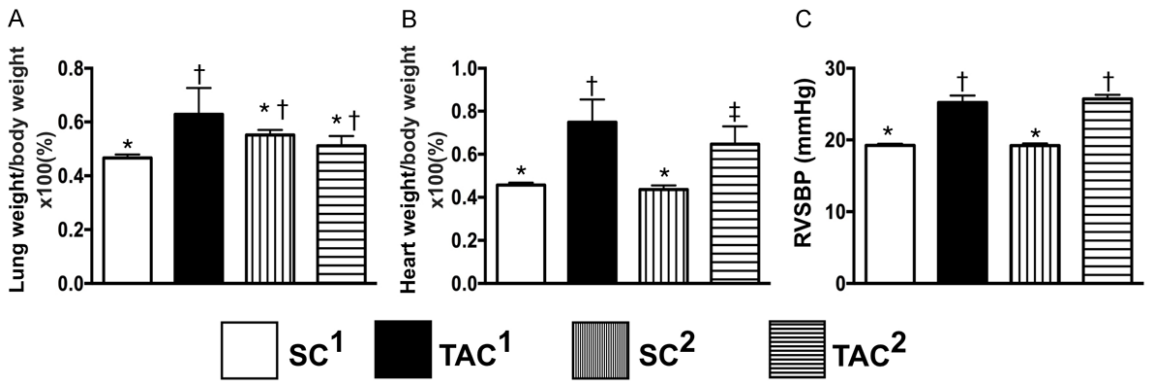

Figure 1. The ratio of heart and lung weight to body weight and right ventricular pressure by day 90 after TAC procedure. A. The ratio of lung weight to body weight, * vs. †, $p < 0.01$. B. Ratio of heart weight to body weight, * vs. other groups with different symbols (‡, ‡), $P < 0.001$. C. The right-ventricular systolic blood pressure (RVSBP), * vs. †, $P < 0.001$. All statistical analyses were performed by one-way ANOVA, followed by Bonferroni multiple comparison post hoc test (n = 10 for each group). Symbols (*, †, ‡) indicate significance (at 0.05 level). SC^1 = sham control of wild-type C57BL/6 (B6) mice; (TAC^1) = SC^1 + transverse aortic constriction; SC^2 = $tPA^{-/-}$/$MMP\text{-}9^{-/-}$ double knockout (DKO) mice; TAC^2 = SC^2 + transverse aortic constriction.

by incubation in secondary antibody solution (1:300) for 1 hour at room temperature. The washing procedure was repeated eight times within 40 minutes. Immunoreactive bands were visualized by enhanced chemiluminescence (ECL; Amersham Biosciences, Amersham, UK) which was then exposed to Biomax L film (Kodak, Rochester, NY, USA). For quantification, ECL signals were digitized using Labwork software (UVP, Waltham, MA, USA). For oxyblot protein analysis, a standard control was loaded on each gel.

Statistical analysis

Quantitative data are expressed as means ± SD. Statistical analysis was adequately performed by ANOVA, followed by Bonferroni multiple-comparison post hoc test. Independent t test was performed for comparison of continuous variables between two groups. SAS statistical software for Windows version 8.2 (SAS institute, Cary, NC) was utilized. A *P* value of less than 0.05 was considered statistically significant.

Results

*Time courses of transthoracic echocardiographic findings (**Table 1**)*

The baseline LVEF, LV factional shortening (FS), interventricular septal thickness, posterior wall thickness, LVEDd and LVESd did not differ among the four groups. However, by days 28, 60 after TAC procedure, the LVEF and LV fractional shortening were significantly higher in SC^1 and SC^2 (i.e., baseline data) than those in TAC^1 and TAC^2 and significantly higher in TAC^2 than those in TAC^1, but there were no significant differences between SC^1 and SC^2. Additionally, by day 90 after TAC procedure, these two parameters were still significantly higher in SC^1 and SC^2 than those in TAC^1 and TAC^2 but there were no notable differences between the former two groups and between the latter two groups.

The interventricular septal thickness and posterior wall thickness were significantly lower in SC^1 and SC^2 than those in TAC^1 and TAC^2 by days 28, 60 and 90 after TAC procedure, but these two parameters did not differ between the former and later two groups.

Furthermore, the LVEDd and LVESd were significantly lower in SC^1 and SC^2 than those in TAC^1 and TAC^2 by days 28, 60 and 90 after TAC procedure. Moreover, these two parameters were significantly higher in TAC^1 than those in TAC^2 by days 28 and 60 after TAC procedure. However, there were no significant differences in the two parameters between TAC^1 and TAC^2 by day 90 after TAC induction, suggesting that DKO did not persistently inhibit LV remodeling compared to that in the wide-type animals in the setting of TAC-induced hypertrophic cardiomyopathy.

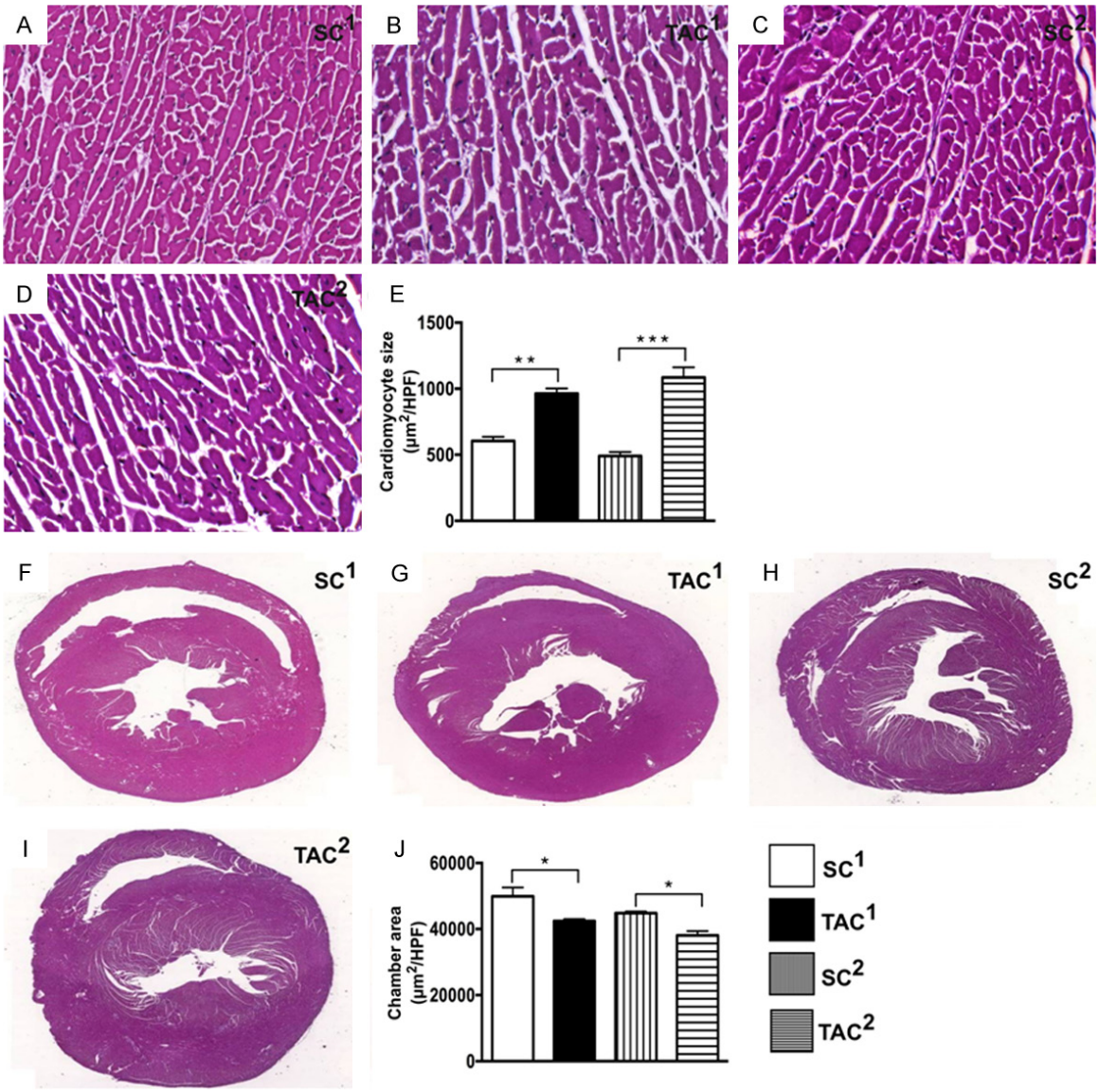

Figure 2. The cardiomyocyte size and LV chamber area by day 90 after TAC procedure. A-D. Illustrating the H.E stain (400 ×) of left ventricular (LV) cross-section for determining cardiomyocyte size. E. Analytical result of cardiomyocyte size, **indicated $P < 0.001$. F-I. illustrating the pathological finding of cross-section of whole heart (40 ×) for identification of LV chamber area of each group at the same cross-section level. J. Analytical result of LV chamber area, *indicated $P < 0.05$. n = 4 for each group. SC^1 = sham control of wild-type C57BL/6 (B6) mice; TAC^1 = SC^1 + transverse aortic constriction; SC^2 = $tPA^{-/-}$/$MMP\text{-}9^{-/-}$ double knockout (DKO) mice; TAC^2 = SC^2 + transverse aortic constriction.

*Heart and lung weights and right ventricular pressure by day 90 after TAC procedure (**Figure 1**)*

By day 90 after the TAC procedure, the ratio of total lung weight to the body was significantly higher in TAC^1 than that in SC^1 but it did not differ among the SC^1, SC^2 and TAC^2 or between TAC^1 and TAC^2. However, the ratio of total heart weight to the body weight was significantly lower in SC^1 and SC^2 than that in TAC^1 and TAC^2 and significantly higher in TAC^1 than that in TAC^2 but no notable difference was noted between SC^1 and SC^2. Additionally, by day 90 after the TAC procedure, the right ventricular systolic blood pressure (RVSBP), an indirect indicator of pulmonary arterial systolic blood pressure, was significantly lower in SC^1 and SC^2 than that in TAC^1 and TAC^2 but there was no significant difference between the former two groups or the latter two groups.

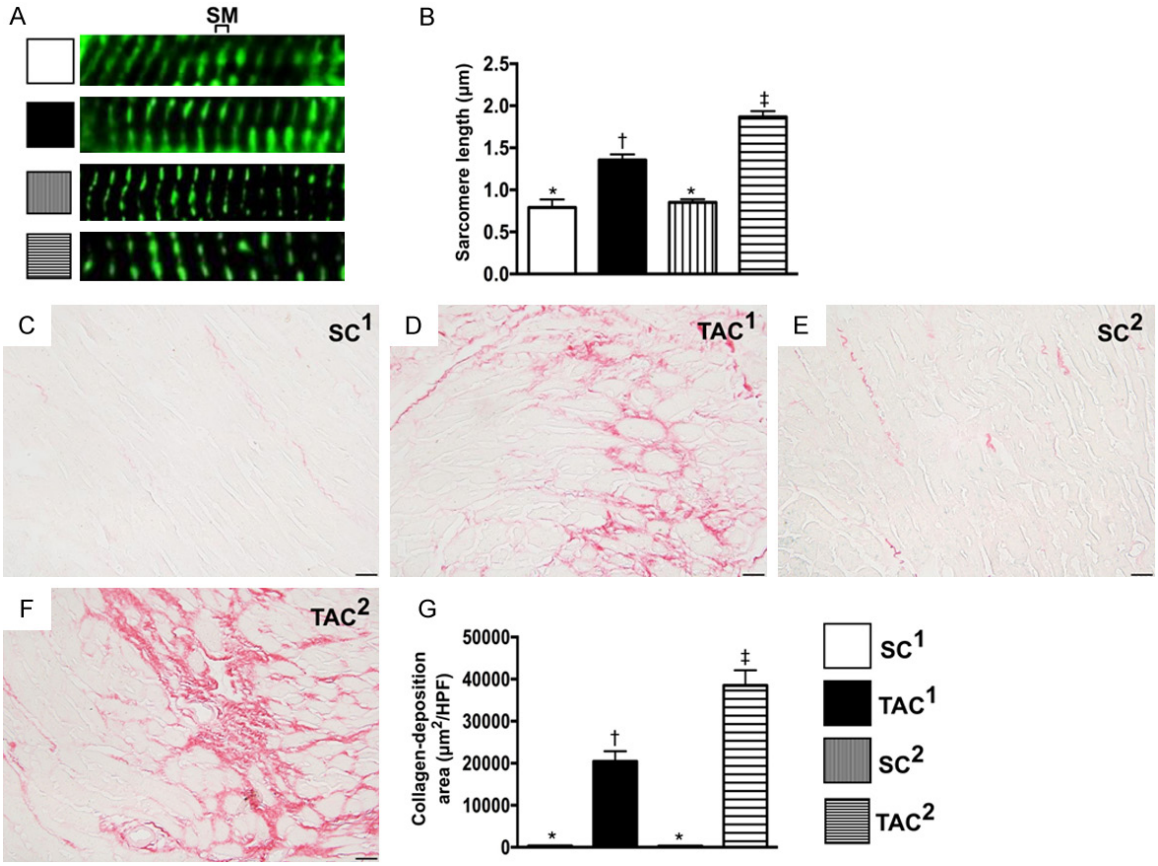

Figure 3. Sarcomere length and condensed collagen-deposition area in LV myocardium by day 90 after TAC procedure. A. Illustrating the immunofluorescent (IF) microscopic finding (1000 ×) for identification of sarcomere (SM) length. B. Analytical result of SM length, * vs. other groups with different symbols (‡, ‡), $P < 0.0001$. C-F. Illustrating the microscopic finding (400 ×) of Sirius red stain for identification of condensed collagen-deposition area. G. Analytical result of condensed collagen-deposition area, * vs. other groups with different symbols (‡, ‡), $P < 0.0001$. Scale bars in right lower corner represent 20 μm. All statistical analyses were performed by one-way ANOVA, followed by Bonferroni multiple comparison post hoc test (n = 6 for each group). Symbols (*, †, ‡) indicate significance (at 0.05 level). SC^1 = sham control of wild-type C57BL/6 (B6) mice; TAC^1 = SC^1 + transverse aortic constriction; SC^2 = $tPA^{-/-}$/$MMP\text{-}9^{-/-}$ double knockout (DKO) mice; TAC^2 = SC^2 + transverse aortic constriction.

*Cardiomyocyte size and LV chamber area by day 90 after TAC procedure (**Figure 2**)*

The cardiomyocyte size was significantly larger in TAC^1 than that in SC^1 and in TAC^2 than in that of SC^2. Additionally, LV chamber size was significantly larger in SC^1 and than in TAC1 and SC^2 than that in TAC^2.

*Sarcomere length and condensed collagen-deposition area in LV myocardium by day 90 after TAC procedure (**Figure 3**)*

The sarcomere length of LV myocardium was significantly increased in TAC^2 than that in SC^1, SC^2 and TAC^1 and significantly increased in TAC^1 than that in SC^1 and SC^2 but no significant difference was noted between the latter two groups, suggesting that by day 90 after TAC procedure DKO did not attenuate the distension of LV myocardium in the present experimental setting of TAC-induced hypertrophic cardiomyopathy.

Sirius red staining demonstrated that the condensed collagen-deposition area, an indicator of accumulation of ECM, was significantly increased in TAC^2 than that in SC^1, SC^2 and TAC^1 and significantly increased in TAC^1 than that in SC^1 and SC^2 but there was no notable difference between the latter two groups, indicating an increase in collagen deposition area in LV myocardium as a result of double gene knockout.

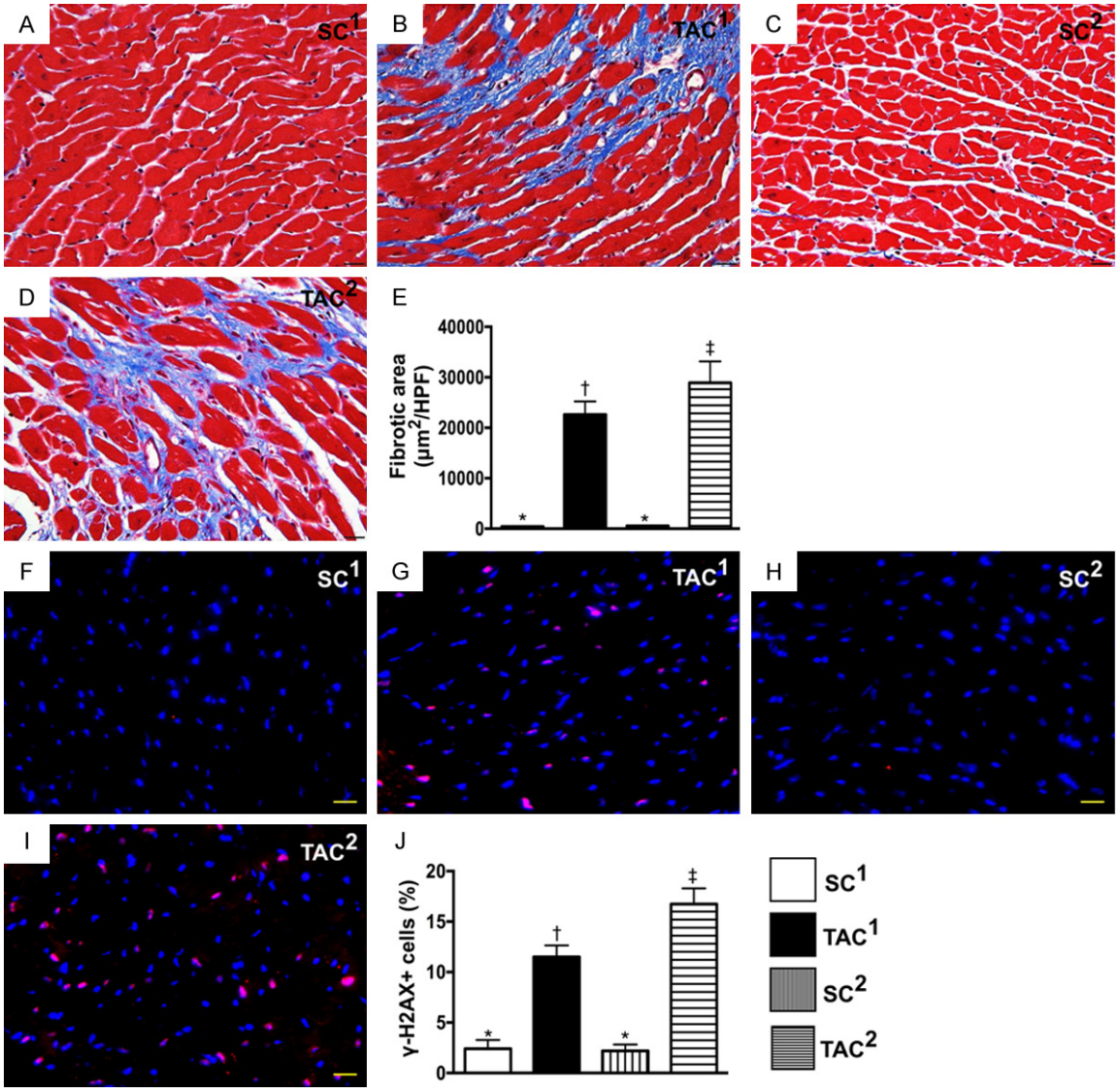

Figure 4. Fibrosis and DNA-damaged biomarker in LV myocardium by day 90 after TAC procedure. A-D. Illustrating the microscopic finding (400 ×) of Masson's trichrome stain for identification of fibrotic area (blue color). E. Analytical result of fibrotic area, * vs. other groups with different symbols (‡, ‡), $P < 0.0001$. F-I. Showing the immunofluorescent microscopic findings (400 ×) for identifying the cellular expression of γ-H2AX (pink color). J. Analytical result of number of γ-H2AX+ cells, * vs. other groups with different symbols (‡, ‡), $P < 0.0001$. Scale bars in right lower corner represent 20 μm. All statistical analyses were performed by one-way ANOVA, followed by Bonferroni multiple comparison post hoc test (n = 6 for each group). Symbols (*, †, ‡) indicate significance (at 0.05 level). SC^1 = sham control of wild-type C57BL/6 (B6) mice; TAC^1 = SC^1 + transverse aortic constriction; SC^2 = $tPA^{-/-}/MMP\text{-}9^{-/-}$ double knockout (DKO) mice; TAC^2 = SC^2 + transverse aortic constriction.

*Expressions of fibrosis and DNA damage biomarker in LV myocardium by day 90 after TAC procedure (**Figure 4**)*

Masson's trichrome staining revealed that the fibrotic area of LV myocardium was significantly increased in TAC^2 than that in SC^1, SC^2 and TAC^1, and significantly increased in TAC^1 than that in SC^1 and SC^2 but no difference was found between the latter two groups. Besides, IF microscopic finding showed that the cellular expression of γ-H2AX, an indicator of DNA damage, exhibited a pattern identical to that of fibrosis among the four groups.

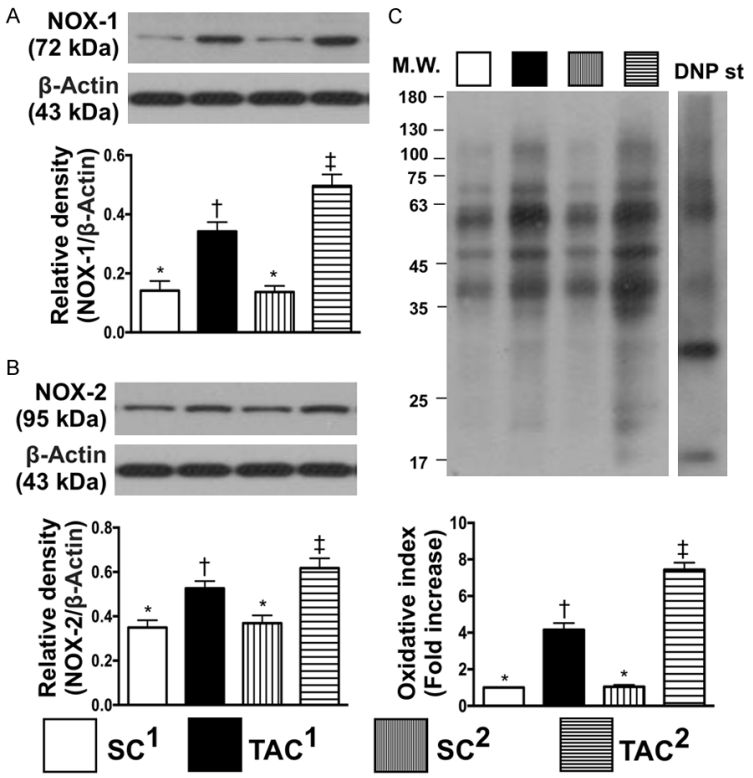

Figure 5. The protein expression of oxidative stress in LV myocardium by day 90 after TAC procedure. A. Protein expression of NOX-1, * vs. other groups with different symbols (‡, ‡), $P < 0.0001$. B. Protein expressions of NOX-2, * vs. other groups with different symbols (‡, ‡), $P < 0.001$. C. Oxidized protein expression, * vs. other groups with different symbols (†, ‡), $P < 0.0001$. (Note: left and right lanes shown on the upper panel represent protein molecular weight marker and control oxidized molecular protein standard, respectively). M.W = molecular weight; DNP = 1-3 dinitrophenylhydrazone. All statistical analyses were performed by one-way ANOVA, followed by Bonferroni multiple comparison post hoc test (n = 6 for each group). Symbols (*, †, ‡) indicate significance (at 0.05 level). SC^1 = sham control of wild-type C57BL/6 (B6) mice; TAC^1 = SC^1 + transverse aortic constriction; SC^2 = $tPA^{-/-}/MMP\text{-}9^{-/-}$ double knockout (DKO) mice; TAC^2 = SC^2 + transverse aortic constriction.

*The protein expression of oxidative stress in LV myocardium by day 90 after TAC procedure (**Figure 5**)*

The protein expressions of NOX-1, NOX-2 and oxidize protein, three indicators of oxidative stress, were significantly higher in TAC^2 than those in SC^1, SC^2 and TAC^1 and significantly increased in TAC^1 than those in SC^1 and SC^2 without notable difference between the latter two groups.

*Protein expressions of apoptotic and fibrotic biomarkers in LV myocardium by day 90 after TAC procedure (**Figure 6**)*

The protein expressions of mitochondrial Bax, cleaved PARP and cleaved caspase 3, three indices of apoptosis, were significantly increased in TAC^2 than those in SC^1, SC^2 and TAC^1 and significantly increased in TAC^1 than those in SC^1 and SC^2 without notable difference between the latter two groups. Additionally, the protein expressions of Smad3 and TGF-β, two indicators of fibrosis, showed an identical pattern compared to that of apoptosis among the four groups.

*The protein expressions of MMPs, inhibitor of TIMPs and inflammatory biomarkers in LV myocardium by day 90 after TAC procedure (**Figure 7**)*

The protein expression of MMP-2 was significantly higher in TAC^2 than that in SC^1, SC^2 and TAC^1 and significantly higher in TAC^1 than that in SC^1 and SC^2 but it showed no difference between the latter two groups. In addition, the protein expression of MMP-9 was significantly higher in TAC^1 than in SC^1 but it was not detected in SC^2 and TAC^2, suggesting that this is result of double gene knockout. On the other hand, the protein expression of TIMP-2 was significantly higher in SC^1 and SC^2 than that in TAC^1 and TAC^2, and significantly higher in TAC^1 than that in TAC^2 but there was no notable difference between TAC^1 and TAC^2. Furthermore, the protein expressions of TNF-α and NF-κB, two indicators of inflammation, exhibited an opposite pattern compared to that of MMP-2 in all groups of animals.

*The protein expressions of DNA/mitochondrial damage, pressure/volume overloaded biomarkers in LV myocardium by day 90 after TAC procedure (**Figure 8**)*

The protein expression of γ-H2AX, a DNA damage biomarker, was significantly higher in TAC^1 and TAC^2 than that in SC^1 and SC^2, and significantly higher in TAC^2 than that in TAC^1 but there was no remarkable difference between SC^1 and SC^2.

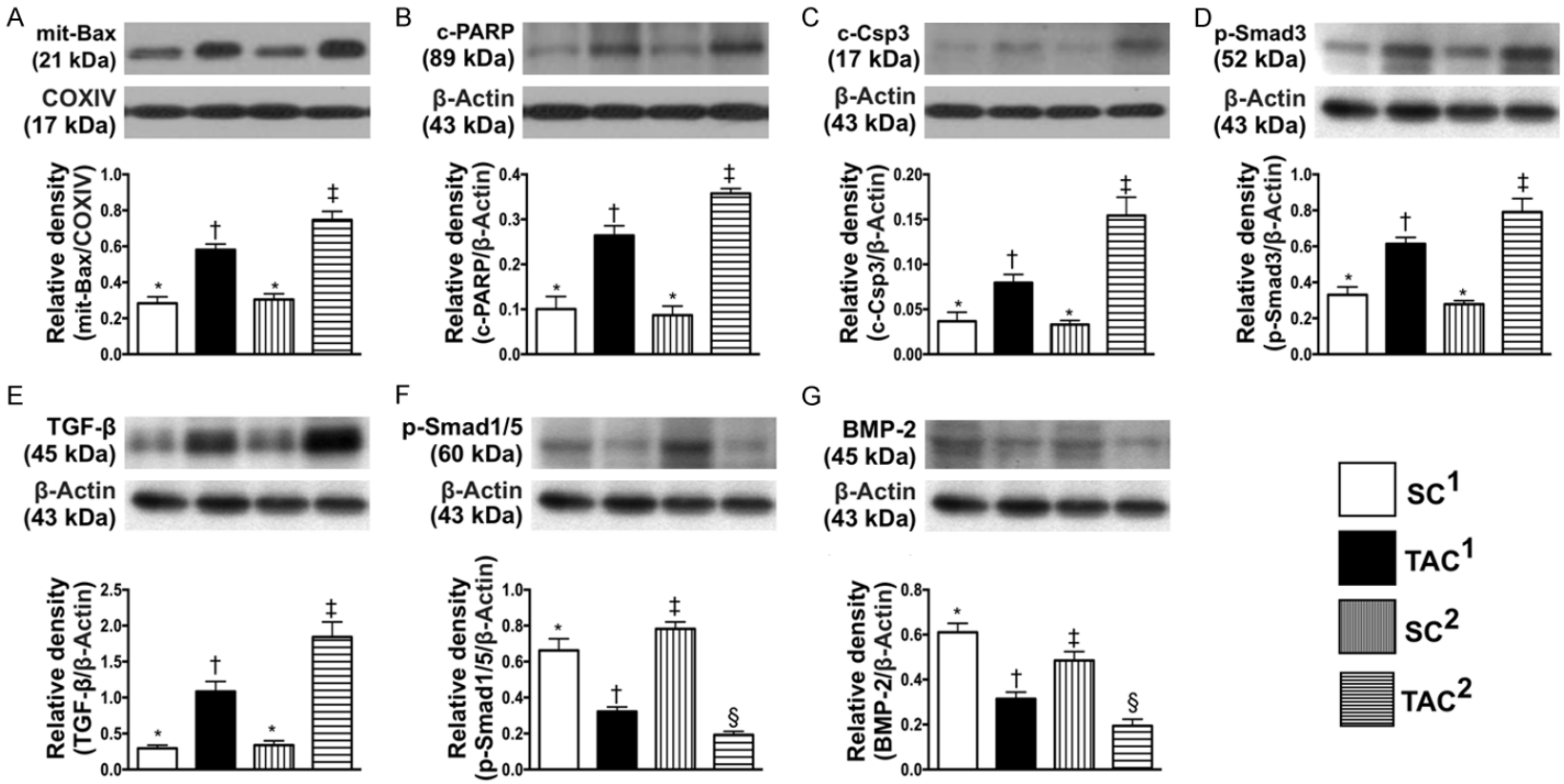

Figure 6. Protein expression of apoptotic and fibrotic biomarkers in in LV myocardium by day 90 after TAC procedure. A. Protein expression of mitochondrial Bax (mit-Bax), * vs. other groups with different symbols (‡, ‡), $P < 0.0001$. B. Protein expression of cleaved, cleaved PARP and cleaved poly (ADP-ribose) polymerase (c-PARP), * vs. other groups with different symbols (‡, ‡), $P < 0.0001$. C. Protein expression of cleaved caspase 3 (c-Csp3), * vs. other groups with different symbols (‡, ‡), $P < 0.0001$. D. Protein expression of phosphorylated (p)-Smad3, * vs. other groups with different symbols (‡, ‡), $P < 0.0001$. E. Protein expression of transforming growth factor (TGF)-β, * vs. other groups with different symbols (‡, ‡), $P < 0.0001$. F. Protein expression of p-Smad1/5, * vs. other groups with different symbols (‡, ‡, §), $P < 0.0001$. G. Protein expression of bone morphogenetic protein (BMP)-2, * vs. other groups with different symbols (‡, ‡, §), $P < 0.0001$. All statistical analyses were performed by one-way ANOVA, followed by Bonferroni multiple comparison post hoc test (n = 6 for each group). Symbols (*, †, ‡, §) indicate significance (at 0.05 level). SC^1 = sham control of wild-type C57BL/6 (B6) mice; TAC^1 = SC^1 + transverse aortic constriction; SC^2 = $tPA^{-/-}/MMP\text{-}9^{-/-}$ double knockout (DKO) mice; TAC^2 = SC^2 + transverse aortic constriction.

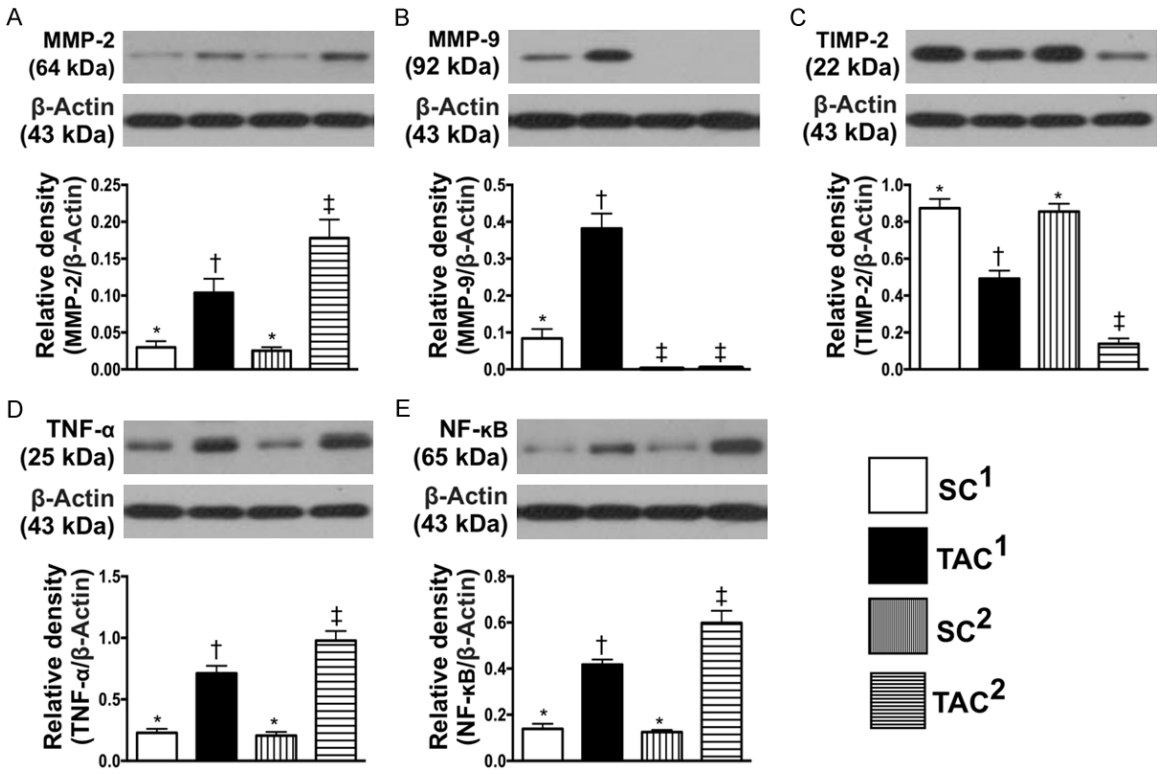

Figure 7. Protein expressions of MMPs, inhibitor of TMIPs and inflammatory biomarkers in in LV myocardium by day 90 after TAC procedure. A. Protein expression of matrix metalloproteinase (MMP)-2, * vs. other groups with different symbols (‡, ‡), P < 0.0001. B. Protein expression of MMP-9, * vs. other groups with different symbols (‡, ‡), P < 0.0001. C. Protein expression of tissue inhibitors of metalloproteinase (TIMP)-2, * vs. other groups with different symbols (‡, ‡), P < 0.0001. D. Protein expression of tumor necrosis factor (TNF)-α, * vs. other groups with different symbols (‡, ‡), P < 0.0001. E. Protein expression of nuclear factor (NF)-κB, * vs. other groups with different symbols (‡, ‡), P < 0.0001. All statistical analyses were performed by one-way ANOVA, followed by Bonferroni multiple comparison post hoc test (n = 6 for each group). Symbols (*, †, ‡) indicate significance (at 0.05 level). SC^1 = sham control of wild-type C57BL/6 (B6) mice; TAC^1 = SC^1 + transverse aortic constriction; SC^2 = $tPA^{-/-}$/$MMP\text{-}9^{-/-}$ double knockout (DKO) mice; TAC^2 = SC^2 + transverse aortic constriction.

The protein expression of cytosolic cytochrome C, an indicator of mitochondrial damage, showed a pattern identical to that of γ-H2AX among the four groups. On the other hand, the protein expression of mitochondrial cytochrome C, an index of integrity of mitochondria, exhibited an opposite pattern compared to that of cytosolic cytochrome C in all groups.

It is well known that cardiac hypertrophy is characterized by a switch from α- to β-MHC protein expression (i.e., reactivation of fetal gene program). In the present study, we found that the protein expressions of BNP and β-MHC, two indicators of pressure-volume overload biomarkers, showed a pattern identical to that of γ-H2AX among the four groups. On the other hand, the protein expression of α-MHC was significantly higher in SC^1 and SC^2 than those of TAC^1 and TAC^2, and significantly higher in TAC^1 than in TAC^2 but it showed no difference between SC^1 and SC^2.

Discussion

This study, which investigated the role of an increase in ECM in myocardium (i.e., resulted from $tPA^{-/-}$/$MMP\text{-}9^{-/-}$ in mice), yielded several striking implications. First, double gene knockout could offer additional benefits in ameliorating the LV remodeling and preservation of LV function in the present experimental setting at the chosen time points (i.e., by days 28 and 60). Second, by day 90 after TAC procedure, LV function and chamber size (i.e., measured by echocardiography) were found to be identical between TAC^1 (i.e., wild-type mice) and TAC^2 (i.e., DKO mice) groups but the ratio of heart

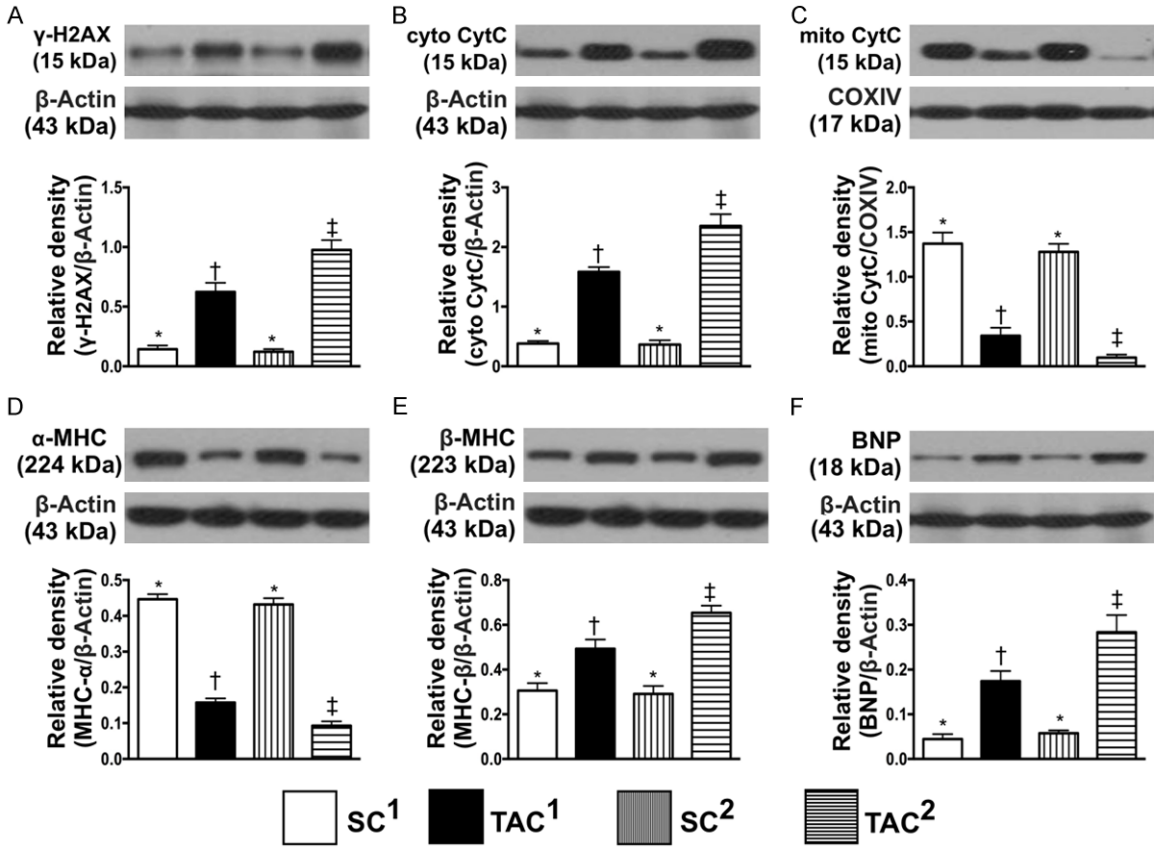

Figure 8. Protein expressions of DNA/mitochondrial damaged, pressure/volume overloaded biomarkers in LV myocardium by day 90 after TAC procedure. A. Protein expressions of γ-H2AX, * vs. other groups with different symbols (‡, ‡), P < 0.0001. B. Protein expression of cytosolic cytochrome C (cyto CytC), * vs. other groups with different symbols (‡, ‡), P < 0.0001. C. Protein expression of mitochondrial cytochrome C (mito CytC), * vs. other groups with different symbols (‡, ‡), P < 0.0001. D. Protein expression of alpha myosin heavy chain (α-MHC), * vs. other groups with different symbols (‡, ‡), P < 0.0001. E. Protein expression of ß-MHC, * vs. other groups with different symbols (‡, ‡), P < 0.001. F. Protein expression of brain natriuretic peptide (BNP), * vs. other groups with different symbols (‡, ‡), P < 0.0001. All statistical analyses were performed by one-way ANOVA, followed by Bonferroni multiple comparison post hoc test (n = 6 for each group). Symbols (*, †, ‡) indicate significance (at 0.05 level). SC^1 = sham control of wild-type C57BL/6 (B6) mice; TAC^1 = SC^1 + transverse aortic constriction; SC^2 = $tPA^{-/-}/MMP\text{-}9^{-/-}$ double knockout (DKO) mice; TAC^2 = SC^2 + transverse aortic constriction.

weight to body weight was significantly higher in TAC^1 than that in TAC^2, suggesting that the capacity for intrinsic LV hypertrophy in response to late stage of TAC-induced pressure overload was better in the former than that in the latter. Third, by day 90 after TAC procedure, the molecular-cellular perturbations of LV myocardium were significantly aggravated in TAC^2 compared to those in TAC^1.

Currently, there has been no investigation addressing whether the presence of accumulated ECM in LV myocardium would offer a positive or negative impact on heart function and LV remolding in the setting of hypertrophic cardiomyopathy. The most important finding in the present study is that, by days 28 and 60 after TAC induction, LV function was preserved and LV chamber dilatation (i.e., index of LV remodeling) was significantly inhibited in TAC^2 animals compared to those in the TAC^1 group, suggesting that DKO offered short-term (i.e., by day-28 after TAC) and intermediate-term (i.e., by day-60 after TAC) protection against TAC-induced hypertrophic cardiomyopathy. Surprisingly, long-term (i.e., day-90 after TAC) LV function and LV chamber dimension were identical between TAC^2 and TAC^1, implying that the protective effect of DKO would disappear after a prolonged period in the present experimental setting.

An association among sarcomere length, LV chamber size, and heart weight has been clearly identified in our previous studies [26, 27]. An essential finding in the present study is that the ratio of total heart weight to body weight was significantly lower in TAC^2 than that in TAC^1 by day 90 after TAC procedure. On the other hand, the sarcomere was significantly longer in TAC^2 than that in TAC^1. The results, in addition to being consistent with the findings of our previous studies [26, 27], may partially explain the deterioration of LVEF and increase of LVEDd/LVESd in TAC^2 and a further increased LVEF and reduced LVEDd/LVESd in TAC^1 at day 90 compared with those at day 60 after TAC induction (**Table 1**).

In the present study, the ratio of lung weight to body weight was similar among the four groups. Additionally, RVSBP, which was less than 30 mmHg in TAC^1 and TAC^2, did not differ between the two groups. These findings imply that we only created a mild pressure overload which may help account for the zero mortality for all animals by day 90 after the TAC procedure.

The association of deterioration in heart function with fibrosis and apoptosis of LV myocardium has been well reported in previous experimental studies [21, 26, 27]. A principal finding in the present study is the remarkably aggravated fibrosis and condensed collagen deposition in TAC^2 compared to those in TAC^1. Additionally, the protein expressions of inflammation, apoptosis, oxidative stress, DNA/mitochondrial damage, and pressure-volume overload biomarkers were notably and consistently up-regulated in TAC^2 compared to those in TAC^1. These findings, in addition to corroborating those of previous studies [21, 26, 27], showed that although $tPA^{-/-}/MMP\text{-}9^{-/-}$ seemed to preserve cardiac function at an early stage (i.e., post-TAC 28 and 60 days) in the present experimental setting of hypertrophic cardiomyopathy, it failed to exert long-term protective effect as reflected in a further reduction in LVEF and an increase in LVEDd/LVESd in TAC^2 animals as well as a preservation of LVEF and a decrease in LVEDd/LVESd in TAC^1 by day 90 compared with those by day 60 after TAC procedure.

Study limitations

This study has limitations. First, since the study period was only 90 days, whether further deterioration of LV function and progression of LV remodeling would develop in TAC^2 animals remain unknown. Second, the mechanisms underlying the rapid deterioration of LVEF and aggravation of remodeling in the TAC^2 animals compared to those in the TAC^1 group at the late stage (i.e., day 90 after TAC) is still unclear.

In conclusion, the results of the present study demonstrated that although genetic knockout of tPA and MMP-9 could offer early protection against hypertrophic cardiomyopathy-induced impairment of cardiac function, it failed to produce long-term protective effects in the present experimental setting.

Acknowledgements

This study was supported by a program grant from Chang Gung Memorial Hospital, Chang Gung University (Grant number: CMRPG8F1851 (1/2), CMRPG8F1852 (2/2)).

Disclosure of conflict of interest

None.

Address correspondence to: Dr. Hon-Kan Yip, Division of Cardiology, Department of Internal Medicine, Kaohsiung Chang Gung Memorial Hospital and Chang Gung University College of Medicine, Kaohsiung 83301, Taiwan. Tel: +886-7-7317123; Fax: +886-7-7322402; E-mail: han.gung@msa.hinet.net; Dr. Hung-I Lu, Division of Thoracic and Cardiovascular Surgery, Department of Surgery, Kaohsiung Chang Gung Memorial Hospital and Chang Gung University College of Medicine, Kaohsiung 83301, Taiwan. Tel: +886-7-7317123; Fax: +886-7-7322402; E-mail: luhung@adm.cgmh.org.tw

References

[1] Azevedo PS, Polegato BF, Minicucci MF, Paiva SA and Zornoff LA. Cardiac remodeling: concepts, clinical impact, pathophysiological mechanisms and pharmacologic treatment. Arq Bras Cardiol 2016; 106: 62-69.

[2] Burchfield JS, Xie M and Hill JA. Pathological ventricular remodeling: mechanisms: part 1 of 2. Circulation 2013; 128: 388-400.

[3] Kehat I and Molkentin JD. Molecular pathways underlying cardiac remodeling during pathophysiological stimulation. Circulation 2010; 122: 2727-2735.

[4] Kerkela R and Force T. Recent insights into cardiac hypertrophy and left ventricular remodeling. Curr Heart Fail Rep 2006; 3: 14-18.

[5] Chan W, Duffy SJ, White DA, Gao XM, Du XJ, Ellims AH, Dart AM and Taylor AJ. Acute left ventricular remodeling following myocardial infarction: coupling of regional healing with remote extracellular matrix expansion. JACC Cardiovasc Imaging 2012; 5: 884-893.
[6] French BA and Kramer CM. Mechanisms of post-infarct left ventricular remodeling. Drug Discov Today Dis Mech 2007; 4: 185-196.
[7] Barison A, Grigoratos C, Todiere G and Aquaro GD. Myocardial interstitial remodelling in non-ischaemic dilated cardiomyopathy: insights from cardiovascular magnetic resonance. Heart Fail Rev 2015; 20: 731-749.
[8] Tayal U and Prasad SK. Myocardial remodelling and recovery in dilated cardiomyopathy. JRSM Cardiovasc Dis 2017; 6: 2048004017734476.
[9] Motoki H, Borowski AG, Shrestha K, Troughton RW, Tang WH, Thomas JD and Klein AL. Incremental prognostic value of assessing left ventricular myocardial mechanics in patients with chronic systolic heart failure. J Am Coll Cardiol 2012; 60: 2074-2081.
[10] Rossi A, Temporelli PL, Quintana M, Dini FL, Ghio S, Hillis GS, Klein AL, Marsan NA, Prior DL, Yu CM, Poppe KK, Doughty RN, Whalley GA; MeRGE Heart Failure Collaborators. Independent relationship of left atrial size and mortality in patients with heart failure: an individual patient meta-analysis of longitudinal data (MeRGE Heart Failure). Eur J Heart Fail 2009; 11: 929-936.
[11] McManus DD, Shah SJ, Fabi MR, Rosen A, Whooley MA and Schiller NB. Prognostic value of left ventricular end-systolic volume index as a predictor of heart failure hospitalization in stable coronary artery disease: data from the heart and soul study. J Am Soc Echocardiogr 2009; 22: 190-197.
[12] Duisters RF, Tijsen AJ, Schroen B, Leenders JJ, Lentink V, van der Made I, Herias V, van Leeuwen RE, Schellings MW, Barenbrug P, Maessen JG, Heymans S, Pinto YM and Creemers EE. miR-133 and miR-30 regulate connective tissue growth factor: implications for a role of microRNAs in myocardial matrix remodeling. Circ Res 2009; 104: 170-178, 6p following 178.
[13] Francia P, Uccellini A, Frattari A, Modestino A, Ricotta A, Balla C, Scialla L and Volpe M. Extracellular matrix remodelling in myocardial hypertrophy and failure : focus on osteopontin. High Blood Press Cardiovasc Prev 2009; 16: 195-199.
[14] Ingle KA, Kain V, Goel M, Prabhu SD, Young ME and Halade GV. Cardiomyocyte-specific Bmal1 deletion in mice triggers diastolic dysfunction, extracellular matrix response, and impaired resolution of inflammation. Am J Physiol Heart Circ Physiol 2015; 309: H1827-1836.
[15] Kitaoka H, Kubo T, Okawa M, Hayato K, Yamasaki N, Matsumura Y and Doi YL. Impact of metalloproteinases on left ventricular remodeling and heart failure events in patients with hypertrophic cardiomyopathy. Circ J 2010; 74: 1191-1196.
[16] Prinz C, Farr M, Laser KT, Esdorn H, Piper C, Horstkotte D and Faber L. Determining the role of fibrosis in hypertrophic cardiomyopathy. Expert Rev Cardiovasc Ther 2013; 11: 495-504.
[17] Tsoutsman T, Wang X, Garchow K, Riser B, Twigg S and Semsarian C. CCN2 plays a key role in extracellular matrix gene expression in severe hypertrophic cardiomyopathy and heart failure. J Mol Cell Cardiol 2013; 62: 164-178.
[18] Yip HK, Yuen CM, Chen KH, Chai HT, Chung SY, Tong MS, Chen SY, Kao GS, Chen CH, Chen YL, Huang TH, Sun CK and Lee MS. Tissue plasminogen activator deficiency preserves neurological function and protects against murine acute ischemic stroke. Int J Cardiol 2016; 205: 133-141.
[19] Yip HK, Sun CK, Tsai TH, Sheu JJ, Kao YH, Lin YC, Shiue YL, Chen YL, Chai HT, Chua S, Ko SF and Leu S. Tissue plasminogen activator enhances mobilization of endothelial progenitor cells and angiogenesis in murine limb ischemia. Int J Cardiol 2013; 168: 226-236.
[20] Lu HI, Huang TH, Sung PH, Chen YL, Chua S, Chai HY, Chung SY, Liu CF, Sun CK, Chang HW, Zhen YY, Lee FY and Yip HK. Administration of antioxidant peptide SS-31 attenuates transverse aortic constriction-induced pulmonary arterial hypertension in mice. Acta Pharmacol Sin 2016; 37: 589-603.
[21] Chen YL, Chung SY, Chai HT, Chen CH, Liu CF, Chen YL, Huang TH, Zhen YY, Sung PH, Sun CK, Chua S, Lu HI, Lee FY, Sheu JJ and Yip HK. Early administration of carvedilol protected against doxorubicin-induced cardiomyopathy. J Pharmacol Exp Ther 2015; 355: 516-527.
[22] Sun CK, Lee FY, Sheu JJ, Yuen CM, Chua S, Chung SY, Chai HT, Chen YT, Kao YH, Chang LT and Yip HK. Early combined treatment with cilostazol and bone marrow-derived endothelial progenitor cells markedly attenuates pulmonary arterial hypertension in rats. J Pharmacol Exp Ther 2009; 330: 718-726.
[23] Sun CK, Lin YC, Yuen CM, Chua S, Chang LT, Sheu JJ, Lee FY, Fu M, Leu S and Yip HK. Enhanced protection against pulmonary hypertension with sildenafil and endothelial progenitor cell in rats. Int J Cardiol 2012; 162: 45-58.
[24] Chen HH, Chen YT, Yang CC, Chen KH, Sung PH, Chiang HJ, Chen CH, Chua S, Chung SY, Chen YL, Huang TH, Kao GS, Chen SY, Lee MS and Yip HK. Melatonin pretreatment enhances the therapeutic effects of exogenous mitochondria against hepatic ischemia-reperfu-

sion injury in rats through suppression of mitochondrial permeability transition. J Pineal Res 2016; 61: 52-68.

[25] Chua S, Lee FY, Chiang HJ, Chen KH, Lu HI, Chen YT, Yang CC, Lin KC, Chen YL, Kao GS, Chen CH, Chang HW and Yip HK. The cardioprotective effect of melatonin and exendin-4 treatment in a rat model of cardiorenal syndrome. J Pineal Res 2016; 61: 438-456.

[26] Lu HI, Chung SY, Chen YL, Huang TH, Zhen YY, Liu CF, Chang MW, Chen YL, Sheu JJ, Chua S, Yip HK and Lee FY. Exendin-4 therapy still offered an additional benefit on reducing transverse aortic constriction-induced cardiac hypertrophy-caused myocardial damage in DPP-4 deficient rats. Am J Transl Res 2016; 8: 778-798.

[27] Lu HI, Lee FY, Wallace CG, Sung PH, Chen KH, Sheu JJ, Chua S, Tong MS, Huang TH, Chen YL, Shao PL and Yip HK. SS31 therapy effectively protects the heart against transverse aortic constriction-induced hypertrophic cardiomyopathy damage. Am J Transl Res 2017; 9: 5220-5237.